




## Cellular automata approach to modeling self-organized periodic patterns in nanoparticle-doped liquid crystals

Piotr Fronczak <sup>1</sup>, Agata Fronczak <sup>1</sup>, Piotr Lesiak <sup>1</sup>, Karolina Bednarska,<sup>1</sup> Wiktor Lewandowski,<sup>2</sup> and Michał Wójcik<sup>2</sup>

<sup>1</sup>*Faculty of Physics, Warsaw University of Technology, Koszykowa 75, PL-00-662 Warszawa, Poland*

<sup>2</sup>*Faculty of Chemistry, University of Warsaw, ul. Pasteura 1, PL-02-093 Warszawa, Poland*



(Received 29 June 2022; accepted 27 September 2022; published 25 October 2022)

Elementary cellular automata provide one of the simplest ways to generally describe the phenomena of pattern formation. However, they are considered too simple to be able to describe in detail the more complex phenomena occurring in real experimental systems. In this article, we demonstrate the application of these methods to optical systems, providing an understanding of the mechanisms behind the formation of periodic patterns in nanoparticle-doped liquid crystals. Our extremely simplified model also explains the observed linear relationship between periodicity and system size.

DOI: [10.1103/PhysRevE.106.044705](https://doi.org/10.1103/PhysRevE.106.044705)

### I. INTRODUCTION

Self-organized pattern formation observed in both natural and technological contexts is a fascinating object of study in various scientific areas including mathematics, physics, biology, chemistry, and computer science. Classical examples are periodic patterns emerging on animal skin such as leopard spots or zebra stripes [1,2], regular thermal fluid convection cells [3], periodic cycles in predator-prey distributions in ecosystems [4], and oscillating chemical reactions such as the Belousov-Zhabotinsky reaction [5,6].

Usually, such phenomena are modeled by nonlinear (sometimes partial) differential equations whose solutions are found by numerical integration. The huge family of models of pattern formation based on reaction-diffusion equations can serve here as a best example [7]. An alternative approach relies on discrete cellular automata (CA) [8]. Among all approaches developed to deal with complexity, CA have the simplest rules that are sufficient to resemble a variety of real emergent patterns and structures. Their main advantage with respect to systems of differential or partial differential equations is the stability of their dynamics. Adding some new features or interactions to the system does not introduce structural instabilities. Such flexibility and computational simplicity make CA an attractive modeling tool for pattern formation phenomena.

To date, many different forms and classes of CA have been developed [9–12]. The simplest ones are one-dimensional elementary CA, which are usually considered “toy models” far from real system dynamics, that only serve for a visual categorization of increasing complexity patterns [8]. In order to analyze real systems, e.g., fluid flows, more sophisticated CA based methods are used, such as the lattice Boltzmann method that closely mimics differential Navier-Stokes equations [9].

Over the past two decades, the formation of self-organizing patterns has been reported in many experimental studies of liquid crystals (LCs) [13–17]. Due to doping them with

nanoparticles, many different textures consisting of stripes or bubbles were obtained as a result of spatial separation of the particle-rich and particle-poor domains. Especially, it has been shown that it is possible to obtain one-dimensional periodic structures spontaneously formed by spatial confinement of a nematic LC doped with gold nanoparticles [17]. The ability to control periodicity of these patterns makes these mixtures attractive from the point of view of the future applications in the information display sector, or in the other optical devices such as low-power-consuming tunable filters or reflectors, light shutters, or electrically controllable intensity modulators. Therefore, modeling such systems, which enables the identification of the most important factors influencing pattern formation, their controllability and stability, is an excellent alternative to expensive laboratory experiments.

LC systems can be mathematically modeled at different levels, ranging from fully molecular approaches [18], through mean-field approaches such as Onsager theory [19] and Maier-Saupe theory [20], to fully continuum approaches such as the Oseen-Frank theory [21], the Ericksen-Leslie theory [22], and the celebrated Landau–de Gennes theory [23]. All of these approaches have their strengths and weaknesses and are used to describe various aspects of the behavior of liquid crystals. However, the complexity of the patterns formed in the LC mixtures eludes the presented formalisms, especially due to its heterogeneity in space. The only exception would be molecular dynamics simulations, but at a high computational cost.

In this paper, we extend the range of available methods used in LC systems to include extremely abstract elementary CA. In this way we show that treating them only as a toy model is too simplistic. Within this approach we model the observed periodic structures in LC mixtures. Creating an automaton with a few simple local rules, we are able to identify all the essential features of the LC system observed in the experiments without having to bother with background details. In particular, our simulations reproduce formation of

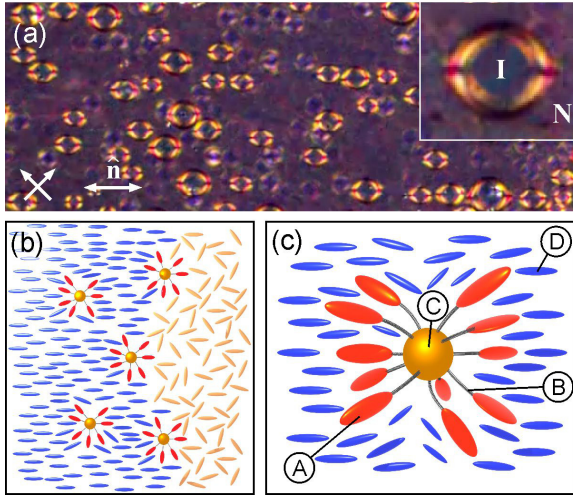


FIG. 1. (a) Optical polarized microscopy image of the two-dimensional LC mixture. The isotropic phase domains that start to nucleate are visible as yellow bubbles. The visible birefringent borders of the isotropic drops with boojums at the poles result from the strong tangential surface anchoring at the isotropic-nematic (I-N) interface. (b) The growing isotropic domain (on the right) pushes the nanoparticles towards the nematic area (on the left). (c) An idealized model of hedgehog-like molecules composed of rigid organic ligands (A) bound by flexible hydrocarbonate chains (B) to the central gold nanoparticle (C) immersed in a nematic liquid crystal (D). Sizes of system elements are not shown to scale.

periodic patterns in a one-dimensional photonic lattice and a continuous change of the structure period during a continuous change of the capillary diameter.

In outline, the paper is as follows. First, we describe shortly the experiment and its main results. Next, we present our CA model. Finally, we discuss the results of the simulation in comparison to the experimental results. The results are supported by a video comparing the process in the simulations vs the real experiment (see Supplemental Material [24]).

**II. EXPERIMENT**

Mixtures of nematic liquid crystals were produced by doping small quantities of gold spherical nanoparticles coated with the longitudinal molecules that bind by flexible hydrocarbonate chains to a central nanoparticle and form together a hedgehog-like complex (see Fig. 1) [17,25]. In the described experiment gold (Au) nanoparticles ( $2.5 \pm 0.4$  nm diameter for the Au core) covered with the promesogenic ligand N,N-dioctyl-4-[(4'-(10-mercaptodecyloxy)-biphenyl-4-yl)oxymethyl]benzamide (2NC8) and LC mixture based on nematics 4-cyano-4'-pentylbiphenyl, commonly referred to as 5CB, were used.

The analysis of an infinite volume sample shows that, as the concentration of nanoparticles increases, the temperature of the nematic-isotropic phase transition also increases. It turns out that in this process nanoparticles act as “anchors” that make it difficult to disrupt the arrangement of LC molecules. Therefore, the transition to the isotropic phase occurs first in regions where the local concentration of nanoparticles is much

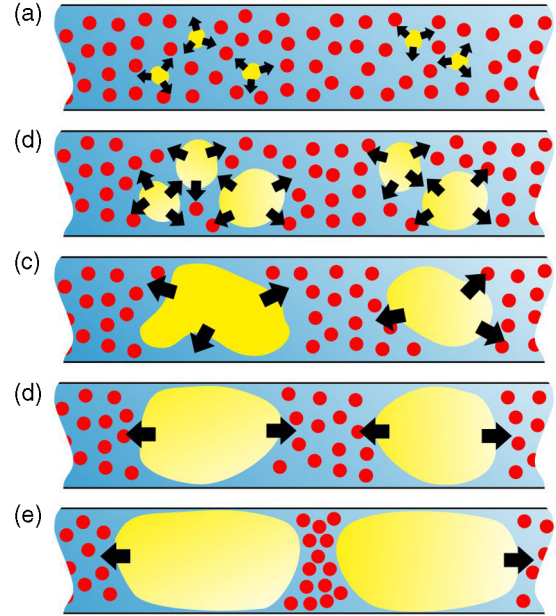


FIG. 2. The process of formation of isotropic domains (yellow shapes) in a mixture of LC and nanoparticles (red dots). Detailed description in the text.

lower than the average, making these places centers of the isotropic domains.

During the experiment, capillaries of various inner diameters were filled with such a mixture. The capillaries were slowly heated, letting the composite material reach the isotropic state. During the heating process, local fluctuations in nanoparticle concentration initiated the formation of isotropic domains. These domains then grew, expelling nanoparticles into adjacent nematic zones. In the first phase of this process, these domains can spontaneously coalesce to form a relatively larger cluster [Figs. 2(b) and 2(c)]. However, when diameters of these domains reach the diameter of the capillary, nanoparticles become trapped between the two growing domains, which leads to a local intense increase in their concentration and ultimately to the excluded volume repulsion of adjacent isotropic domains [Figs. 2(d) and 2(e)], which stops their growth.

There are two experimental observations important for the possible applications. First, it occurs that a one-dimensional (along the capillary) structure of isotropic domains created in the above described stochastic process seems to be periodic (Fig. 3). Second, it has been shown that the period of such a structure depends almost linearly on the capillary diameter [Fig. 6(d)]. In the next section we demonstrate a simple CA that models both these observations.

**III. CELLULAR AUTOMATA MODELING**

In general, a cellular automaton consists of a regular (any-dimensional) grid of cells, each in one of a finite number of states [8]. Initially, one has to assign a state for each cell. Then, a new generation of states is created according to some fixed rule that determines the new state of each cell in terms of the current state of the cell itself and the states of its neighbors.

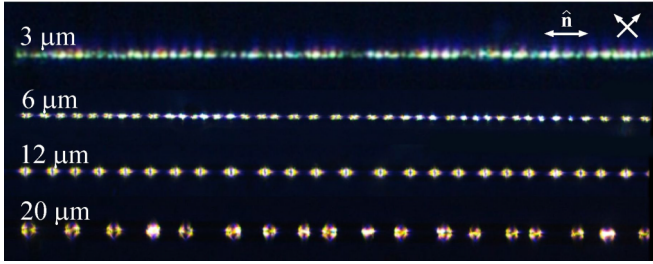


FIG. 3. Periodic patterns obtained in the experiment in capillaries of different widths. The concentration of gold nanoparticles in 5CB liquid crystals was 0.3 wt.%. Photos were taken at a temperature  $T = 35.6^\circ\text{C}$ .

The simplest, elementary cellular automaton (ECA) is a one-dimensional chain of cells where there are two possible states (labeled 0 and 1) and the rule to determine the state of a cell in the next generation depends only on the current state of the cell and its two immediate neighbors. Since there are  $2^3 = 8$  possible current states, there are a total of  $2^8 = 256$  possible ECAs, each of which can be indexed with an 8-bit binary number [8]. Two examples of such ECAs with rules 254 and 222 are shown in the Fig. 4(a) and 4(b).

To model the experiment described earlier, we create the initial state of such an ECA consisting of a random sequence of 1 and 0 sites with probabilities  $p$  and  $1 - p$  respectively, where 1's represent independently formed isotropic domains. The first phase of the process [corresponding to Figs. 2(a)–2(c)] is modeled using the rule 254 shown in Fig. 4(a). This rule produces growing domains that can coalesce into larger clusters. Duration of this phase,  $t_A$  depends on the capillary

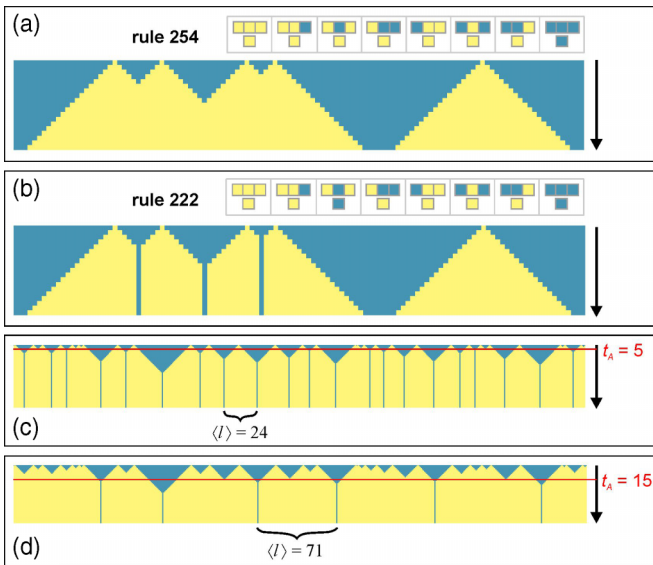


FIG. 4. The diagram of the rule and the first 20 generations of elementary cellular automaton starting with a random initial condition for the rule: (a) 254 and (b) 222. Two realizations of the process of isotropic domains' growth that lead to the formation of the periodic patterns in LC for two values of the model parameter  $t_A = 5$  (c) and  $t_A = 15$  (d). In all subfigures the direction of time is indicated by a black arrow.

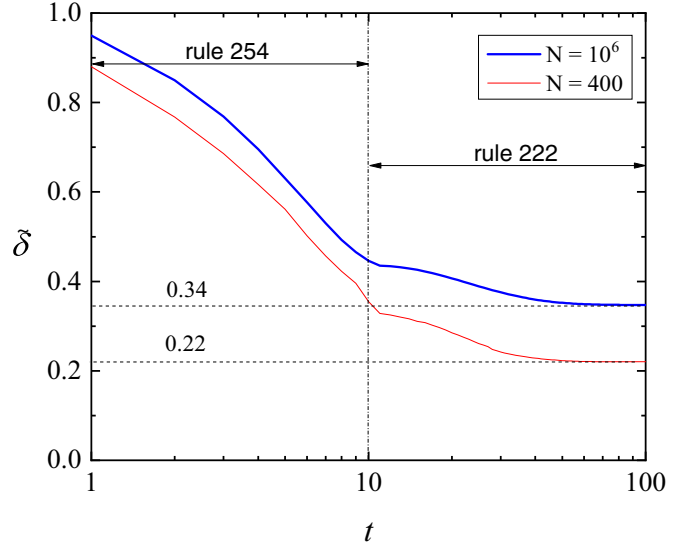


FIG. 5. Normalized standard deviation of the distance,  $\tilde{\delta}$ , as a function of time for  $p = 0.1$  and  $t_A = 10$  in the large system ( $N = 10^6$  cells, blue thick line) and in the small one ( $N = 400$ , red thin line).

diameter  $d$  and it generally increases with  $d$ . After time  $t_A$ , we apply the second rule 222 [cf. Fig. 4(b)], which also supports the growth of domains, but in this case two colliding domains do not merge (which imitates the excluded volume effect). The process ends when all adjacent isotropic domains are separated by one nematic cell (in state 0) and the state of the system does not change. This extremely simple model allows one to simulate all main effects observed in the experiment. For demonstration purposes we show in Figs. 4(c) and 4(d) the full process of the periodic pattern formation for two different times  $t_A$ . The process, compared with the actual behavior of the LC mixture in the experiment, is also shown as a movie in the Supplemental Material [24].

In the following, we will demonstrate in detail, first, how periodicity emerges in a system starting from irregular initial conditions, and second, how the period of the resulting structure depends on the width of the system.

#### IV. RESULTS

To observe how a periodic pattern emerges from completely random initial conditions, at each time step we compute the distance  $l$  between the centers of adjacent domains and its mean value  $\langle l \rangle$ . In Fig. 5 we present the normalized standard deviation of the distance,  $\tilde{\delta}$ , as a function of time for  $p = 0.1$  and  $t_A = 10$  in the large (blue thick line) and in the small system (red thin line).

In the large system (here  $N = 10^6$ ), initially, at time  $t = 1$ , the standard deviation is large. It results from the geometric distribution of the initial distances between the domains,  $\tilde{\delta} = \sqrt{1 - p}$ . In the first phase, for  $t \in [1, t_A]$ ,  $\tilde{\delta}$  decreases sharply. In the second phase, for  $t > t_A$ ,  $\tilde{\delta}$  still decreases, but slower, and goes asymptotically to the finite value  $\tilde{\delta}_{\text{inf}}$ . This value of  $\tilde{\delta}_{\text{inf}} = 0.34$ , obtained for the parameters specified above, allows us to observe quasiperiodic patterns in the automaton.



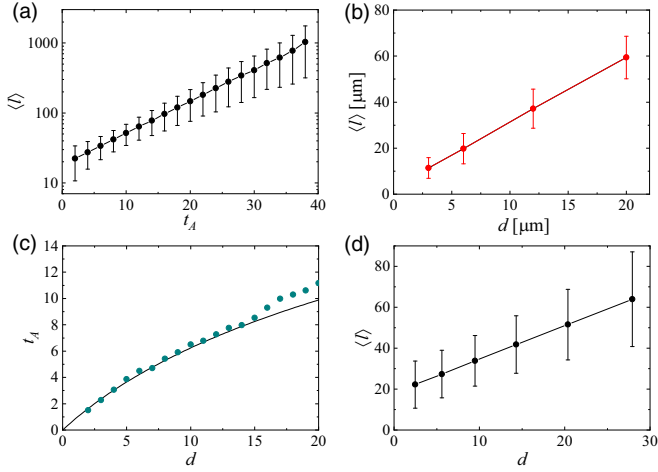


FIG. 6. Dependence of the mean period of the formed structure  $\langle l \rangle$  on (a) the length  $t_A$  of the first phase of the model, (b) the diameter  $d$  of the capillary in the experiment, and (d) the width  $d$  of the capillary in the model. (c) Relation between  $t_A$  and the width  $d$  of the capillary found from the simulation of the two-domain system. The points are averaged over 100 different initial conditions (random vertical positions of domains). The black line represents the empirically found best fit function  $t_A = 9 \ln(d/10 + 1)$ .

However, in the experiment, depending on the sample we found even lower values of  $\tilde{\delta}$ , ranging from 0.15 to 0.25. Assuming that the model correctly describes the phenomenon occurring in the liquid crystal, we see only two possible explanations for this discrepancy.

The first one is a much smaller size of the experimental system, allowing us to obtain only a set of over a dozen distances between domains. This significantly reduces standard deviation. In Fig. 5 for comparison purposes we present also the results obtained for a small system size of  $N = 400$  (red line is an average over an ensemble of 100 different realizations). In this case,  $\tilde{\delta}_{\text{inf}} = 0.22$  is in agreement with actual observations. The second possible explanation comes from the observation that, in the capillary, small domains may disappear due to thermal fluctuations, making the set of interdomain distances more uniform (see the two red arrows in the movie in Supplementary Material). Unfortunately, this effect cannot be achieved with deterministic CA.

In the experiment, it was observed [17] that the period of the obtained structure depends almost linearly on the capillary diameter (see, e.g., Fig. 6(b) or more detailed Fig. 10 in [17]). In order to simulate this phenomenon in our CA model we note that the wider diameter of the capillary corresponds to the longer time  $t_A$  of the first phase. This is simply because in the larger capillary the growing isotropic domain needs more time to reach the medium boundary.

In Fig. 6(a) we show the dependence of the mean period  $\langle l \rangle$  of the periodic pattern on the length  $t_A$  of the first phase of the model. It seems that the growth of  $\langle l \rangle$  is not linear but clearly exponential (note the log-linear scale of the plot). This result, however, cannot be directly compared with the behavior observed in the experiment [Fig. 6(b)], because we do not know how the time  $t_A$  relates to the width of the capillary  $d$  (except that the relation should be increasing).

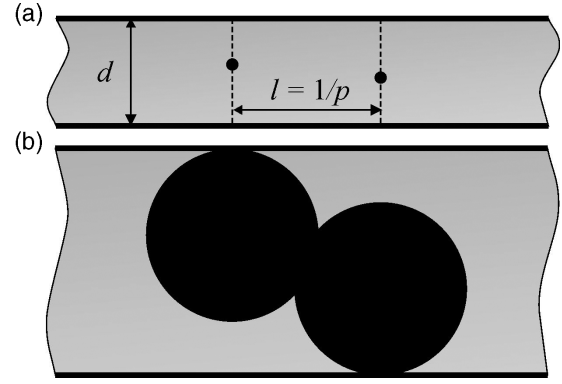


FIG. 7. (a) Schematic illustration of the two just created isotropic domains separated horizontally by distance  $l$ . (b) An example of a situation where two merging domains separate the two sides of a capillary.

To find this relationship, we performed a simple simulation of two growing circular domains in a  $d$ -wide capillary (the *Mathematica* code of the simulation is included in the Supplemental Material [24]). The centers of the domains are horizontally distant by  $l = \frac{1}{p}$ , while their vertical position is completely random. This situation is schematically illustrated in Fig. 7(a). In a simulated process, we measure the time  $t_A$  (averaged over different initial conditions) it takes for growing domains to contact both capillary boundaries as a function of  $d$ . When the capillary is thin, the domains cannot touch each other before the end of the process. However, in the case of a thick capillary, it is possible for the domains to join during growth and separate the two sides of the capillary earlier than if they were two noninteracting domains [see Fig. 7(b)]. The results of the simulation presented in Fig. 6(c) show that the relation between  $t_A$  and  $d$  is sublinear. The empirical logarithmic curve shown there can be used as a guideline. Having this relationship in mind, we can present in Fig. 6(d) the dependence of the mean period  $\langle l \rangle$  on the capillary width  $d$ . The obtained dependence is linear, in a great analogy to the experimental data [Fig. 6(b)].

## V. CONCLUSIONS

A successful model should be as simple as it can be, easy to use, and at the same time detailed enough to provide a good description of the relevant physical situation. In this paper, we believe we present such a model. It is based on the simplest, elementary cellular automaton which realistically resembles a composite material consisting of gold nanoparticles and a nematic liquid crystal matrix that has the ability to self-create a periodic structure in the form of a one-dimensional photonic lattice through a phase separation process occurring in a confined space. We expect that the simplicity of this model will, in the future, facilitate analytical description of the observed process.

## ACKNOWLEDGMENTS

Studies were funded by a FOTECH-1 project granted by Warsaw University of Technology under the program Excellence Initiative: Research University (ID-UB).

- [1] A. M. Turing, The chemical basis of morphogenesis, *Phil. Trans. R. Soc. Lond.* **B237**, 37 (1952).
- [2] H. Meinhardt, *Models of Biological Pattern Formation* (Academic, London, 1982).
- [3] J. Swift and P. C. Hohenberg, Hydrodynamic fluctuations at the convective instability, *Phys. Rev. A* **15**, 319 (1977).
- [4] R. M. May, Limit cycles in predator-prey communities, *Science* **177**, 900 (1972).
- [5] A. M. Zhabotinsky, Periodical process of oxidation of malonic acid solution, *Biophysics* **9**, 306 (1964), in Russian.
- [6] B. F. Madore and W. L. Freedman, Computer simulations of the Belousov-Zhabotinsky reaction, *Science* **222**, 615 (1983).
- [7] M. Cross and H. Greenside, *Pattern Formation and Dynamics in Nonequilibrium Systems* (Cambridge University Press, Cambridge, 2009).
- [8] S. Wolfram, Statistical mechanics of cellular automata, *Rev. Mod. Phys.* **55**, 601 (1983).
- [9] U. Frisch and B. Hasslacher, and Y. Pomeau, Lattice-Gas Automata for the Navier-Stokes Equation, *Phys. Rev. Lett.* **56**, 1505 (1986).
- [10] W. Gilpin, Cellular automata as convolutional neural networks, *Phys. Rev. E* **100**, 032402 (2019).
- [11] W. Dzwiniel, Complex automata as a novel conceptual framework for modeling biomedical phenomena, in *Advances in Intelligent Modelling and Simulation*, edited by A. Byrski, Z. Oplatkova, M. Carvalho, and M. Kisiel-Dorohinicki, Studies in Computational Intelligence, Vol. 416 (Springer, Berlin, 2012).
- [12] S. Wolfram, *A Project to Find the Fundamental Theory of Physics* (Wolfram Media, Champaign, IL, 2020).
- [13] Y. J. Kang, K. J. Erickson, and T. A. Taton, Plasmonic nanoparticle chains via a morphological, sphere-to-string transition, *J. Am. Chem. Soc.* **127**, 13800 (2005).
- [14] C. R. Iacovella and S. C. Glotze, Complex crystal structures formed by the self-assembly of detethered nanospheres, *Nano Lett.* **9**, 1206 (2009).
- [15] O. Benson, Assembly of hybrid photonic architectures from nanophotonic constituents, *Nature (London)* **480**, 193 (2011).
- [16] M. A. Boles, M. Engel, and D. V. Talapin, Self-assembly of colloidal nanocrystals: From intricate structures to functional materials, *Chem. Rev.* **116**, 11220 (2016).
- [17] P. Lesiak *et al.*, Self-organized, one-dimensional periodic structures in a gold nanoparticle-doped nematic liquid crystal composite, *ACS Nano* **13**, 10154 (2019).
- [18] M. P. Allen, Molecular simulation of liquid crystals, *Mol. Phys.* **117**, 2391 (2019).
- [19] L. Onsager, The effects of shape on the interaction of colloidal particles, *Ann. N.Y. Acad. Sci.* **51**, 627 (1949).
- [20] W. Maier and A. Saupe, Eine einfache molekulare theorie des nematischen kristallinflussigen zustandes, *Z. Naturforsch. A* **13**, 564 (1958).
- [21] C. W. Oseen, The theory of liquid crystals, *Trans. Faraday Soc.* **29**, 883 (1933).
- [22] J. L. Ericksen, Liquid crystals with variable degree of orientation, *Arch. Ration. Mech. Anal.* **113**, 97 (1990).
- [23] P. G. de Gennes and J. Prost, *The Physics of Liquid Crystals*, International Series of Monographs on Physics, Vol. 83 (Oxford University Press, Oxford, 1995).
- [24] See Supplemental Material at <http://link.aps.org/supplemental/10.1103/PhysRevE.106.044705> for a video file and the source code of the simulation.
- [25] I. Membrillo Solis, T. Orlova, K. Bednarska *et al.*, Tracking the time evolution of soft matter systems via topological structural heterogeneity, *Commun. Mater.* **3**, 1 (2022).